

# Ground states of a frustrated kagomé array of Josephson junctions

Mohammad R. Kolahchi<sup>1</sup> and Joseph P. Straley<sup>2</sup>

<sup>1</sup>*Institute for Advanced Studies in Basic Sciences, Gava Zang, P. O. Box 45195-159, Zanjan, Iran*

<sup>2</sup>*Department of Physics, University of Kentucky, Lexington, Kentucky 40506*

(Received 13 April 2002; revised manuscript received 20 June 2002; published 14 October 2002)

We study the ground state vortex lattices of a kagomé array of Josephson junctions in an external magnetic field. We give a simple model that accounts for the principal dependence of ground state energy on the density of vortices, and exhibit the exact ground state configurations for a sequence of special values. A Monte Carlo simulated annealing shows that there is very little further structure. For the special case  $f=AB/\Phi_0=1/2$  it is known that there is an infinite degeneracy. We give a numerical technique for evaluating the zero temperature entropy.

DOI: 10.1103/PhysRevB.66.144502

PACS number(s): 74.50.+r, 64.60.-i

## I. INTRODUCTION

A superconducting network in an external magnetic field is a frustrated system.<sup>1</sup> The adjacent superconductors are connected by a Josephson junction, which attains a minimum energy when the phases of neighboring superconductors differ in a way that depends on their relative positions and on the strength of the magnetic field. This optimum phase relationship generally cannot be attained globally, since the sum of the phase differences around any closed loop must be zero (mod  $2\pi$ ). This leads to observable effects: a decoration of the sample by nickel particles indicates a superlattice of magnetic sites,<sup>2,3</sup> visualized as clusters of Ni particles. The magnetic sites are a manifestation of the presence of current vortices, which in turn are a consequence of the long-range superconducting coherence. The square lattice version of this model has been studied by a number of workers<sup>4</sup>; in this case the vortices are believed to generally form a periodic structure at low temperatures.

The kagomé structure is interesting because it contains plaquettes of very different areas. These plaquettes attain their unfrustrated configuration (that  $BA/\Phi_0$  be an integer) at different values of the field, giving a more complex relationship between energy and field than that obtained for Bravais lattices.

In recent experimental and theoretical studies, the fully frustrated kagomé lattice of superconducting wires was found to lack an ordered superlattice. Higgins *et al.*<sup>5</sup> measured the resistance of an aluminum kagomé wire network, and verified the absence of any anomaly for the case of  $1/2$  flux quantum per unit cell, in agreement with the theoretical study of Lin and Nori.<sup>6</sup> The experiments of Pannetier *et al.* on the dual lattice to the kagomé lattice, the so-called dice lattice (or the  $T3$  geometry), have shown the same behavior.<sup>7</sup>

It is believed that the high degeneracy of the fully frustrated state of the kagomé lattice is responsible for this behavior. As almost all of the states in this degenerate manifold are disordered, there is no way for the system to find the commensurate state, unless some other mechanism intervenes. This reasoning is inspired by the knowledge of the ground state properties of the Heisenberg antiferromagnet on a kagomé lattice.<sup>8</sup> The disordered nature of the ground states in the degenerate manifold has also led to the investigation

of the possible glassy characteristics. This is specially interesting, because such spin systems are inherently without disorder.<sup>9</sup>

Here we study the ground state properties of the frustrated planar rotor model on the kagomé lattice.<sup>10</sup> This model describes an array of Josephson junctions, assuming that only the phase of the superconducting order parameter is allowed to fluctuate. In Sec. II, we describe this model, and in Sec. III we present a general scheme for studying the ground state configurations. In Sec. IV, we study the ground states at various values of the vortex density, focussing on the cases where a simple periodic structure is available. In Sec. V, we discuss the special case  $f=1/2$ , where an infinite degeneracy occurs. Section VI gives a summary of results.

## II. KAGOMÉ LATTICE

A kagomé lattice is a collection of corner-sharing triangles, as shown in Fig. 1. The unit cell contains two equilateral triangles and one hexagon. There are two bonds per site of the kagomé lattice, and three sites per unit cell.

Usually it is convenient to measure the external magnetic field in terms of flux quanta per unit cell. However, in the present case it is better to use a different scale, by defining  $f=AB/\Phi_0$ , where  $A$  is the area of the triangular plaquette, and  $\Phi_0=ch/2e$  is the flux quantum. For a given value of the external magnetic field, this definition yields values for  $f$  which are numerically eight times smaller than the usual definition (because the triangle is  $1/8$  of a unit cell).

The Josephson junction array is constructed such that the

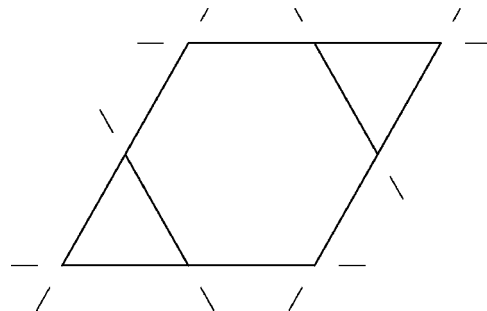


FIG. 1. The unit cell for the kagomé structure.

sites of the kagomé lattice are occupied by the superconducting islands, and each bond carries a Josephson junction. Let  $\langle ij \rangle$  denote the bond connecting two nearest neighbors  $i$  and  $j$ . The phase of the superconducting order parameter at the superconducting island  $i$  is denoted by  $\theta_i$ . Due to the presence of a magnetic field perpendicular to the plane of the lattice, this phase is rotated by an amount determined by the line integral of the vector potential along the bond  $\langle ij \rangle$ :

$$\chi_{ij} = \frac{2e}{c\hbar} \int_i^j \vec{A}(\vec{r}) \cdot d\vec{l}. \quad (1)$$

The Hamiltonian is given by

$$H = -J \sum_{\langle ij \rangle} \cos(\theta_i - \theta_j - \chi_{ij}), \quad (2)$$

where the coupling constant  $J$  is taken to be positive.

Increasing  $f$  by unity adds one flux quantum to each triangle and six flux quanta to the hexagons, which can be gauged out of Eq. (2) by redefining  $\theta_i$ . The Hamiltonian is also invariant under the reversal of the field direction. This allows us to restrict our study to  $f$  in the interval  $[0, 1/2]$  (the choice of scale for  $f$  was made for this reason). However, there is an energy cost to having a nonintegral multiple of flux quanta in a plaquette.

The phase field  $\{\theta_i\}$  accommodates the frustration introduced by  $A_{ij}$  by introducing singular points which are the equivalents of the vortices in type-II superconductors (and will be called vortices in what follows). The presence of these vortices can be revealed by introducing the gauge-invariant phase differences

$$v_{ij} = (\theta_i - \theta_j - \chi_{ij})/2\pi - (\text{integer}), \quad (3)$$

where the integer is chosen so that  $-\frac{1}{2} < v_{ij} < \frac{1}{2}$ , and then computing the vorticity

$$V = \sum v_{ij}, \quad (4)$$

where the sum is over the edges of a plaquette. If  $v_{ij}$  are slowly varying, the phase differences cancel out in the sum, leaving just the flux measured in units of the flux quantum—specifically  $V = -f$  for triangular plaquettes and  $V = -6f$  for hexagonal plaquettes. However, for plaquettes containing a vortex,  $V$  differs from this by an integer. We observe that this result can be restated as meaning that there is a “background” vorticity  $-f$  per triangle (a hexagon contains six triangles), and then a vortex confers integer vorticity to its plaquette.

There is another way to characterize the vortices. Each link of the network carries a supercurrent directed from site  $i$  to site  $j$ ,

$$\mathcal{J}_{ij} = \mathcal{J} \sin(2\pi v_{ij}), \quad (5)$$

where  $\mathcal{J} = 2eJ/\hbar$  is the critical current for a link. Now we may define the circulation

$$C = \sum \sin(2\pi v_{ij}), \quad (6)$$

again summing over the edges of the plaquette. Well away from any vortex, the  $v_{ij}$  are small [to minimize Hamiltonian (2)], and then the circulation and the vorticity agree. However, they differ near the vortex core: the circulation is altered there, and in rare circumstances will describe the vortex as being delocalized over several plaquettes, while the vorticity must assign the vortex to some particular plaquette. The circulation is a more physical variable, while the vorticity gives a better representation of the mathematical constraints.

When  $f$  is rational, the  $\chi_{ij}$  are periodic (modulo  $2\pi$ ), and then the phase field and vortex pattern can also be periodic on a superlattice. Only in this case can the system exhibit superconductivity: the breaking of translational symmetry prevents flux flow. Thus we restrict our attention to the case when  $f = p/q$  is a rational fraction. A special property of this case is that the directed sums of  $v_{ij}$  and  $\sin(2\pi v_{ij})$  around the boundary of a periodicity cell necessarily vanish (since every link and its periodic image contribute in opposite sense), and thus we have a pair of rules, that the sum of  $V$  and the sum of  $C$  over all plaquettes in a periodicity cell are both zero.

### III. INDEPENDENT VORTEX MODEL

The ground state of the system on any type of lattice, kagomé or otherwise, is a particular set of phases  $\theta_i$  that minimizes the energy of the entire lattice, as given by Eq. (2). Although there are no isolated plaquettes in a lattice, it is a remarkable empirical finding that for rational values of  $f$  the system distributes the phases so that nearly all the plaquettes act as if isolated in achieving the minimum energy. This constitutes the independent-vortex model.

Now consider the case of isolated plaquettes—triangles or hexagons—without external connections. A triangular plaquette minimizes its energy to

$$E = -3J \cos\left(\frac{2\pi(f^\# - f)}{3}\right), \quad (7)$$

where  $f^\#$  is the integer nearest to  $f$ , while the minimal energy for a hexagonal plaquette is

$$E = -6J \cos\left(\frac{2\pi(F^\# - 6f)}{6}\right), \quad (8)$$

where  $F^\#$  is the integer nearest to  $6f$ . The corresponding vorticity is  $f^\# - f$  for triangles, and  $F^\# - 6f$  for hexagons. Figure 2 shows how the energy per site of the isolated plaquette depends on  $f$  for the interval  $0 < f < \frac{1}{2}$ .

We observe that within this range the lowest energy state for the triangle is always  $f^\# = 0$ , while for the hexagon it is  $F^\# = 0, 1, 2$  or  $3$ , depending on the value of  $f$ . However, the situation becomes complicated because the vorticity sum rule prevents us from putting all the plaquettes into their lowest energy state. According to Fig. 2, it costs less energy to change the vorticity of a hexagon than to introduce a triangle of excited vorticity, except for the interval  $0.435 < f < \frac{1}{2}$ . This suggests that over much of the range of  $f$ , the vortices are resident only on the hexagons, so that the ground state con-

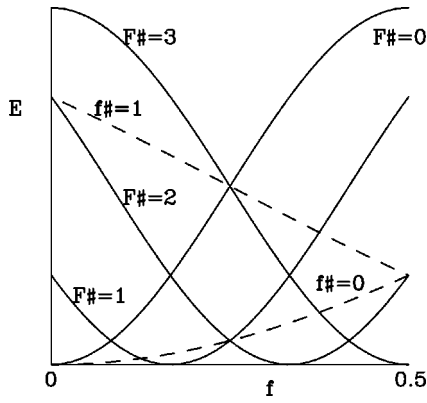


FIG. 2. Energies of vortex configurations.

figurations will tend to resemble those of the hexagonal geometry; only close to  $f = \frac{1}{2}$  will the triangle vortices be observed.

Explicitly, let us assume that for some value of  $f < 0.435$  a fraction  $X$  of the hexagons in a large region contain vortices characterized by an integer  $F\#$ , while the remaining fraction  $(1-X)$  contain vortices characterized by  $F\# + 1$ , and that all triangles remain in the state  $f\# = 0$ . Then the vorticity sum rule implies

$$X(F\# - 6f) + (1-X)(F\# + 1 - 6f) - 2f = 0, \quad (9)$$

giving simply  $X = (F\# + 1 - 8f)$ . The energy per site can then be calculated by adding Eqs. (7) and (8) for the appropriate values of  $F\#$  and  $f\#$ , with the indicated weightings.

For the case  $0.435 < f < \frac{1}{2}$  we can proceed in a similar manner, except that now the minimum energy (subject to the vorticity sum rule) is given by putting all the hexagons into the  $F\# = 3$  state, and letting a fraction  $Y$  of the triangles be in the  $f\# = 1$  state. An argument similar to the one above gives  $Y = 8f - 3$ .

Putting together the various cases gives Fig. 3. The cusps correspond to the cases where only one kind of vortex is observed in the hexagons; in the intervening regions, one kind of hexagon vortex is replaced by another, or triangle vortices are introduced.

The implications of this model for the behavior near  $f = 0.435$  is somewhat unphysical: a finite density of hexagon

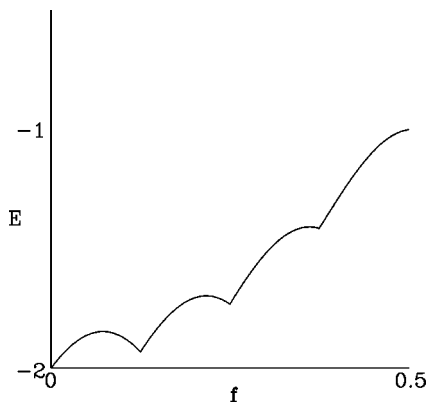
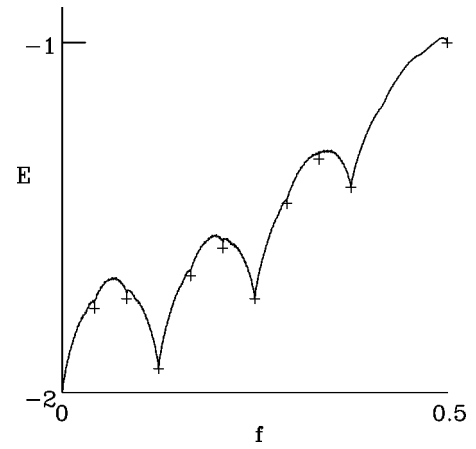


FIG. 3. Energies of vortex configurations.

FIG. 4. Dependence of the energy per site on the flux density, for  $0 < f < \frac{1}{2}$ . The + markers indicate exact results.

vortices with  $F\# = 4$  is abruptly replaced by a finite density of triangle vortices with  $f\# = 1$ . This unrealistic outcome is a consequence of ignoring the interactions between vortices, which is mediated by the overlap of their current patterns. The discontinuous behavior gives rise to no visible anomaly in Fig. 3, because the energy cost of adding a vortex to a triangle or to a hexagon is exactly the same at  $f = 0.435$ .

#### IV. PERIODIC VORTEX STRUCTURES

Figure 4 reports the ground state energy of a kagomé lattice of Josephson junctions as a function of  $f$ , constructed by a Metropolis Monte Carlo simulated annealing on a rhombic cell with periodic boundary conditions containing  $50 \times 50$  unit cells. This permits  $f$  to be sampled in steps of size 0.005. We also considered the special cases  $f = \text{integer}/24$ , using a  $48 \times 96$  unit cell.

Simulated annealing gives a useful upper bound and estimate for the ground state energy. However, the true ground state configurations for this system are periodic, and it is unlikely that this would result from a simulated annealing run. We can offer two kinds of validation for the Monte Carlo study: the dependence on  $f$  is fairly smooth, with no discontinuities; and the Monte Carlo results are systematically and uniformly slightly higher than the exact energies, in the cases that these are known. We have spot checked the Monte Carlo annealing by constructing periodic vortex structures; these agree to within 1%. Thus we believe Fig. 4 gives a good idea how the ground state energy varies with flux density.

The most prominent features in Fig. 4 are the cusps that occur for  $f = 1/8, 1/4$ , and  $3/8$ —and then the slightly surprising lack of any feature at  $f = 1/2$ . The cusps correspond to states in which all triangles are in vorticity state  $f\# = 0$  and all hexagons are also in the same vorticity state (where there are three choices  $F\# = 1, 2$ , or  $3$ ). For these cases every bond of the network is carrying the same current  $\sin(2\pi F\#/24)$ , exactly as if the vortices were isolated;<sup>11</sup> the energy density is  $E = -2 \cos(2\pi f/3)$ . Inspection of the ground states for other values of  $f < 3/8$  confirms that these can be described as a low density of hexagons characterized by one value of

$F\sharp$ , within a background of hexagons characterized by a different value, with all triangles in the  $f\sharp=0$  state. These observations are consistent with the simple model that led to Fig. 3. However, we note that except at the special values  $f=n/8$ , Fig. 3 gives energy that is significantly lower, because that model ignores the inconsistent assignment of currents by hexagons and by triangles.

Figure 4 also differs from Fig. 3 by the presence of smaller features at intermediate values of  $f$ , such as at  $f = \frac{1}{24}, \frac{1}{12}, \frac{1}{6}, \frac{5}{24}$ , and  $\frac{7}{24}$ . These can be described as periodic arrangements of the different vorticity sites with a supercell that contains three unit cells of the kagomé structure. In the study of the square lattice structure,<sup>10</sup> it was found that for every  $f=p/q$  the lowest energy structure was a periodic arrangement of the vortices, with a supercell was a periodic arrangement of the vortices. The supercell frequently had the area of  $q$  unit cells (the exceptions were twice as large). We suspect that the kagomé structure for  $8f=P/Q$  may also be periodic, with a supercell whose area is  $Q$  times larger than the kagomé unit cell. The square lattice study<sup>10</sup> also found that the energy is slightly lower when  $q$  is small (so that  $f$  is a simple rational fraction), but that these cusps rapidly decrease in size with  $q$ . The implications for the present work are that increased annealing effort would reveal further cusps for small  $Q$ , but that these would lead only to a slight roughening of the curve in Fig. 4.

This structure in the dependence of the energy on  $f$  arises because the energy depends on the current distribution in a way that is well approximated by saying that the vortices interact as if they were particles carrying integer-valued charge (as specified by  $F\sharp$  or  $f\sharp$ ), with a neutralizing background charge density  $-f$  per triangle. The vorticity sum rule then becomes the expected statement of overall charge neutrality, and the lowest energy configurations will be those that give the most uniform distribution of vortices. For cases when  $f$  is a simple rational fraction, this is accomplished by a periodic structure; for other values of  $f$ , the periodicity is at best large scale, implying a larger ‘‘Coulombic’’ energy. The most important qualification to this model is that the energy is more closely associated with the circulation than with the vorticity, so that the charge of a vortex is actually somewhat delocalized over neighboring plaquettes—especially in the case of the triangle vortices.

An interesting set of nontrivial structures arises when we decorate the  $\sqrt{3} \times \sqrt{3}$  superlattice, with one hexagon having  $F\sharp=M$  and two having  $F\sharp=M \pm 1$  (an example is shown in Fig. 5). The unit supercell contains three unit cells of the original structure (shown in Fig. 1), and thus nine kagomé sites and the area of 24 triangles. The vorticity sum rule requires that the explicit vorticity contributed by the hexagons be canceled by the background vorticity provided by the magnetic field, implying  $M+2N=24f$ . Symmetry dictates that the currents on the six sides of any hexagon are the same, resulting in an expression for the energy per site:

$$E = -\frac{6}{9} \cos 2\pi \left( \frac{M}{6} - f \right) - \frac{12}{9} \cos 2\pi \left( \frac{N}{6} - f \right). \quad (10)$$

The values for  $f$  and the corresponding energies are given in Table I below.

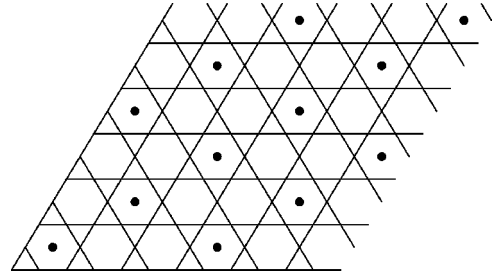


FIG. 5. Vortex arrangement for the ground state for  $f=1/6$ . The triangles are all in the state  $f\sharp=0$ , while the hexagons are in states  $F\sharp=1$  (with no current on their boundaries) and 2 (with current  $J\sqrt{3}/2$ ). Dots have been drawn in the hexagons with  $F\sharp=2$  vorticity.

Other arrangements of the vortices can be constructed with nearly the same energy. However, with the exception of the case  $f=10/24$  these appear to be the arrangements that make the density of vortices most uniform, which results in the lowest energy.

As suggested by the independent vortex model, for  $f > 3/8$  we expect the hexagons to all be in the same state  $F\sharp=3$ , while the triangles having an appropriate density in  $f\sharp=1$ . For example, consider the cases  $f=2/5$  and  $f=5/12$ . The ground states are shown in Figs. 6 and 7. The structure for  $f=5/12$  shown in Fig. 7 has an energy of  $-1.184$ , slightly lower than the candidate structure given in the last line of Table I.

As noted above, the triangle vortices are somewhat more delocalized (in terms of their circulation pattern) than for the hexagons. As a consequence, the total energy is less sensitive to the local arrangement of these vortices, and the true ground state is not so readily distinguished from a large set of nearly degenerate alternatives. However, we believe the ground state configuration to be unique, and that we have correctly identified them.

In the study of ground state vortex lattices as a function of frustration parameter, one usually gives importance to the vortex lattices that can be commensurate with the underlying lattice structure. This means, for example, that a vortex superlattice with a unit cell of size  $8 \times 8$  cannot be observed on a  $50 \times 50$  underlying grid. In practice, however, it is easier to

TABLE I. Values of  $f$  and  $E$  for the  $\sqrt{3} \times \sqrt{3}$  Bravais structures.

$M$	$N$	$f$	$E$	$E$
1	0	$\frac{1}{24}$	$-(\sqrt{8} + \sqrt{6})/3$	-1.7593
0	1	$\frac{2}{24}$	$-\sqrt{3}$	-1.732
1	1	$\frac{3}{24}$	$-(3 + \sqrt{3})/\sqrt{6}$	-1.9319
2	1	$\frac{4}{24}$	$-5/3$	-1.6667
1	2	$\frac{5}{24}$	$-(\sqrt{6} + 5\sqrt{2})/6$	-1.5868
2	2	$\frac{6}{24}$	$-\sqrt{3}$	-1.7321
3	2	$\frac{7}{24}$	$-(3\sqrt{6} + \sqrt{2})/6$	-1.4604
2	3	$\frac{8}{24}$	$-4/3$	-1.3333
9	3	$\frac{9}{24}$	$-\sqrt{2}$	-1.4142
4	3	$\frac{10}{24}$	$-2/\sqrt{3}$	-1.1547

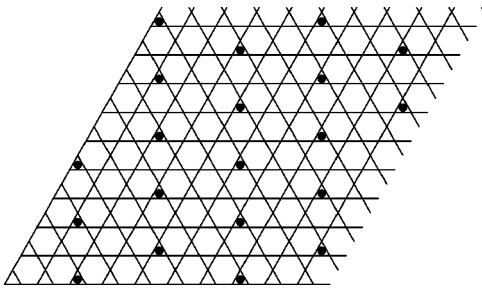


FIG. 6. The ground state for  $f=2/5$ . All hexagons contain  $F\# = 3$  vortices. The triangles containing a vortex are marked by a black dot. The energy of this structure is  $-1.2363$ .

identify such a vortex lattice than one with a unit cell of size  $25 \times 25$ , despite the commensuratness of the latter. Physically, the reason is attributed to the fact that a larger unit cell means coherence over larger areas, which is only achieved at lower temperatures. A larger unit cell usually corresponds to  $f=p/q$  with larger  $q$ , so it can be approximated by other  $f$  having smaller denominators. This, in turn, makes the search for the “correct” vortex structure more cumbersome.

V. SPECIAL CASE  $f=1/2$

An interesting feature of Fig. 4 is that it looks smoother as  $f=1/2$  is approached. The general reason for the presence of a cusp is the existence of a ground state that has a simple periodicity, which can happen if  $f=p/q$  is a rational fraction composed of small integers.

Clearly there are not very many states of this type. In the study of the square lattice version of this problem<sup>10</sup> the ground states for other  $f$  were found to consist of alternating domains of regions characterized by other values of  $f$ . If the domain wall energies are not small, there will necessarily be a cusp at the special values. Since  $f=1/2$  is a very simple fraction indeed, it is surprising that there is no singularity here; it implies that the domain wall energy is small, or that the ground state is not unique.

In fact it is known that  $f=1/2$  has an infinite set of ground states,<sup>11</sup> so that this particular case has finite entropy at  $T=0$ . In outline, the argument is that the Josephson ground states are characterized by having every link carry the same current  $(\sqrt{3}/2)J$  and thus make the same contribution  $-\frac{1}{2}J$  to the total energy. This implies that the “gauge invariant phase differences” [Eq. (3)] always have the single value  $2\pi/3$ , and then the configurations can be uniquely described

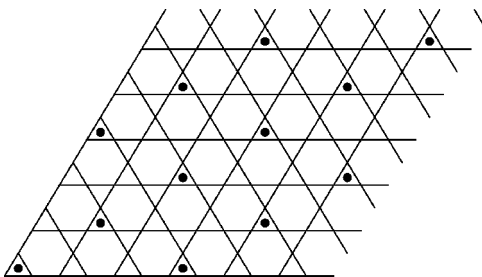


FIG. 7. The ground state for  $f=5/12$ . The representation is the same as in Fig. 6.

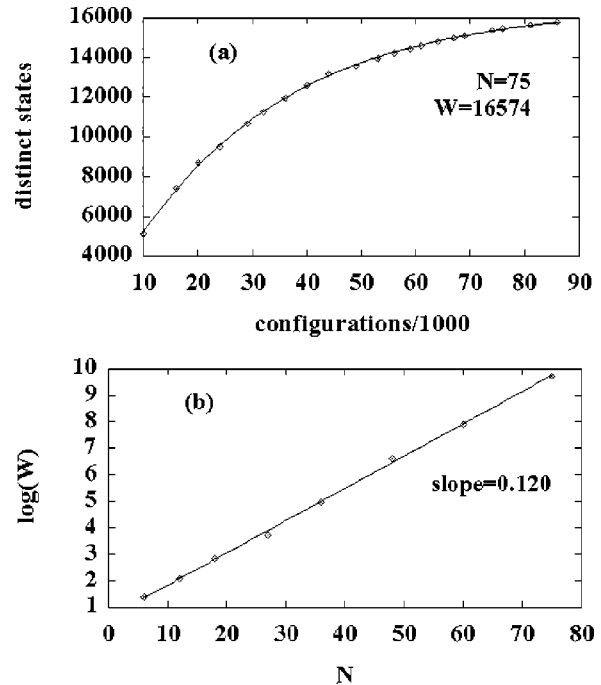


FIG. 8. Determining the zero point entropy. (a) The number of distinct vortex lattices is found for kagomé lattices with 6, 12, 18, 27, 36, 48, 60, and 75 kagomé sites. The data for the largest lattice are shown (a). The asymptote gives  $W$  for  $N=75$ . (b) How the number of configurations  $W$  depends on size  $N$ .

by indicating the orientation of the bonds.<sup>12</sup> For a consistent assignment of phases there are a number of constraints on the bond orientations—in particular, the currents on any triangle circulate either to right or left, assigning a definite chirality to it.

Under these conditions, we can transform one ground state configuration into many others by identifying a path along which the currents alternate in direction, and then reversing the orientation of all these currents, and the chirality of the associated triangles. In every configuration there are at least  $\mathcal{O}(N)$  possible paths, so that by repeating this transformation we perform a random walk in a configuration space of very high dimensionality, leading to the possibility of a finite ground state entropy. Elser<sup>11</sup> and Huse and Rutenberg<sup>13</sup> showed that this problem is equivalent to the previously studied<sup>14</sup> case of the antiferromagnetic three-component Potts model (also on the kagomé lattice), for which the zero point entropy per site is known to be 0.126.

In order to show that this result has meaning for the Josephson network, as well as to demonstrate how to determine the zero point entropy for problems Baxter has not yet solved, we devised a numerical estimate of the zero point entropy. A Metropolis Monte Carlo simulation was run at the low temperature  $T=0.001$  on finite lattices. This generated a sequence of configurations, which included a number that had energy very close to the ground state energy; these all satisfied the known constraints (i.e., all triangles had a definite chirality) and were accepted as examples of ground state configurations. A list of these configurations was kept, and it was noted how many of these were distinct in the sense that

they assigned different chirality to some of the triangles. It was found that the number  $D$  of distinct configurations grew with the total number  $A$  of accepted ground state configurations according to the rule

$$D = D_{\text{inf}} - ce^{-kA}. \quad (11)$$

By fitting the data to this form (using only the larger values of  $A$ ) an estimate was obtained for the total degeneracy  $D_{\text{inf}}$ . Figure 8(a) shows this relationship for the case of a finite system of 75 kagomé sites (the largest value that was considered). The estimate for the ground state degeneracy of this size lattice is  $D_{\text{inf}}(75) = 16574$ . The resulting estimates of the dependence of the ground state degeneracy on lattice size was in turn fit to the relationship  $\alpha N = \ln[D_{\text{inf}}(N)]$ , as shown in Fig. 8(b), with the result  $\alpha \sim 0.120$ . We think the similarity

between this estimate and the known exact value to be rather promising.

## VI. SUMMARY

We have shown that the major features of the energy dependence can be accounted for in terms of the independent vortex model, and by means of a Monte Carlo simulated annealing, shown that this model gives a fairly good representation, even for the cases that  $f$  is a ratio of small integers. We have checked this simulation by exhibiting the exact ground state for several special values. Finally, we have given a numerical route to estimating the degeneracy of the special case  $f = \frac{1}{2}$ .

## ACKNOWLEDGMENTS

M.R.K. would like to thank the Institute for Advanced Studies in Basic Sciences, Zanjan, for their support and encouragement of this project.

<sup>1</sup>B. Pannetier, A. Bezryadin, and A. Eichenberger, *Physica B* **222**, 253 (1996).

<sup>2</sup>J.P. Straley, *Phys. Rev. B* **38**, 11 225 (1988).

<sup>3</sup>The Abrikosov flux lattice is the well known example of such magnetic sites. Unlike the Abrikosov flux lines, here the vortices do not have a core. However, an experimental technique which greatly improves the detection of the vortices, turns the vortex lattice into an Abrikosov lattice (see Ref. 1).

<sup>4</sup>J. Villain, *J. Phys. C* **10**, 4793 (1977); S. Teitel and C. Jayaprakash, *Phys. Rev. B* **27**, 598 (1983).

<sup>5</sup>M.J. Higgins *et al.* *Phys. Rev. B* **61**, R894 (2000).

<sup>6</sup>Y.-L. Lin and F. Nori, *Phys. Rev. B* **50**, 15 953 (1994).

<sup>7</sup>B. Pannetier, C.C. Abilio, E. Serret, T. Fourier, P. Butaud, and J. Vidal, *Physica C* **352**, 41 (2001); [cond-mat/0005254 (unpublished)].

<sup>8</sup>J. Villain *et al.* *Phys. (Paris)* **41**, 1263 (1980); J.T. Chalker, P.C.W. Holdsworth, and E.F. Shender, *Phys. Rev. Lett.* **68**, 855 (1992); A. Chubukov, *ibid.* **69**, 832 (1992); R. Moessner and J.T.

Chalker, *ibid.* **80**, 2929 (1998); B. Canals and C. Lacroix, *ibid.* **80**, 2933 (1998).

<sup>9</sup>G. Aeppli and P. Chandra, *Science* **275**, 5297 (2000).

<sup>10</sup>For such a study on the square lattice, see J.P. Straley and G.M. Barnett, *Phys. Rev. B* **48**, 3309 (1993).

<sup>11</sup>V. Elser, *Phys. Rev. Lett.* **62**, 2405 (1989).

<sup>12</sup>Although every vortex configuration corresponds to a particular directed kagomé graph, the reverse is not at all true—most directed graphs have no interpretation in terms of the Josephson model.

<sup>13</sup>D.A. Huse and A.D. Rutenberg, *Phys. Rev. B* **45**, 7536 (1992).

<sup>14</sup>R.J. Baxter, *J. Math. Phys.* **11**, 784 (1970). The problem solved in this paper is equivalent to ours. A positive vertex is one that if we circle it clockwise, the three bond colors  $A$ ,  $B$ , and  $C$  appear in even order; a negative vertex has them in odd order. The final result  $\log(1.20872 \dots)$  needs to be adjusted by a factor of  $2/3$ , which is the ratio of the number of sites of the honeycomb lattice (number of triangle vortices in the kagomé lattice) to the number of sites in the kagomé lattice, giving  $0.12637 \dots$